Full Title: Structural and mechanistic diversity in p53-mediated regulation of organismal

longevity across taxonomical orders

Short Title: p53 and organismal longevity

Romani Osbourne[1,2][¶][*] , Kelly M. Thayer[2][¶]

[1] Department of Molecular Biology & Biochemistry, Wesleyan University, Middletown,

Connecticut, United States of America

[2] College of Integrative Sciences, Wesleyan University, Middletown, Connecticut, United

States of America

* Corresponding author

Email: rosbourne@wesleyan.edu

[¶] These authors contributed equally to this work.

Abstract

The accumulation of senescent cells induces several aging phenotypes, and the p53 tumor suppressor protein regulates one of the two known cellular senescence pathways. p53's regulation of senescence is however not clear. For example, p53 deficiency in some mice has been shown to rescue premature aging while others display significant aging phenotype when p53-deficient. This study seeks to elucidate, structurally and mechanistically, p53's roles in longevity. Through a relative evolutionary scoring (RES) algorithm, we quantify the level of evolutionary change in the residues of p53 across organisms of varying average lifespans in six taxonomic orders. Secondly, we used PEPPI to assess the likelihood of interaction between p53–or p53-linked proteins–and known senescence-regulating proteins across organisms in the orders Primates and Perciformes. Our RES algorithm found variations in the alignments within and across orders, suggesting that mechanisms of p53-mediated regulation of longevity may vary. PEPPI results suggest that longer-lived species may have evolved to regulate induction and inhibition of cellular senescence better than their shorter-lived counterparts. With experimental verification, these predictions could help elucidate the mechanisms of p53-mediated cellular senescence, ultimately clarifying our understanding of p53's connection to aging in a multiple-species context.

Author summary

The p53 tumor suppressor protein protects our genome from cancers by repairing DNA damage, regulating cell death and/or pushing cells to a state where they become permanently unable to divide (known as cellular senescence). An accumulation of senescent cells produces various molecular features of aging in both mouse and human cellular models–thus linking p53 to the aging process. However, the molecular mechanism by which p53 regulates aging and its structural implications on this regulation are not clear. In this study, we assessed quantitatively the evolutionary differences in p53 sequences of organisms across several taxonomical orders to determine if there is a relationship between average lifespan and sequence evolution. In addition, we used a protein-protein interaction tool to assess the likelihood of interaction between p53, or p53-associated protein, and various senescence-associated proteins across organisms of various lifespans in two taxonomic orders: Primates and Perciformes. An elucidation of p53 structural difference and mechanistic proteomic network linked to p53 regulation of cellular senescence could advance therapeutics targeting abnormal aging.

Introduction

Usually, aging is a gradual process characterized (in human and mouse models) by molecular biomarkers such as a decrease in leukocyte telomere length, decreased levels of insulin/insulin-like growth factor (IGF-1), and increased inflammation. Several molecular mechanisms have been purported to regulate aging and determine lifespan–many of which have been linked to p53 tumor suppressor activities. In low or high-stress conditions, p53 binds to several target genes–including those that encode promyelocytic leukemia protein (PML), plasminogen activator inhibitor-1 (PAI-1), and deleted in esophageal cancer 1 (DEC1)–which then induce cellular senescence [1,2]. The link between aging and its ability to push cells to senescence is of particular interest to this study. In a senescent state, a damaged cell resists apoptosis and ceases to replicate. An accumulation of these cells triggers the aging process by creating a senescence-associated secretory phenotype (SASP) which creates a chronic inflammatory microenvironment. Chaib et. al. has shown that a programmed clearance of senescent cells delays aging phenotypes [3].

While p53 consensus sequences for most of these targets have been elucidated, few studies have explored regulatory mechanisms and structural features of p53 that could be implicated in organismal aging. Residual changes in the DNA-binding domain of several orthologs of p53 in Cetaceans have been linked to longevity [(4)]. This supports findings that p53-mediated cellular senescence could be mediated directly by DNA binding. Additionally, there has been an extension exploration of the role of the mouse double, minute two (MDM2) gene in the aging process of mice. MDM2 is the most

well-studied negative inhibitor of p53 tumor suppressive activity. Wu et. al. have demonstrated that disruption of the MDM2-p53 axis accelerates aging in some mice [2]. In another study in which nearly all of their p53 N-terminal was deleted, several mice displayed high resistance to cancer, but also shorter lifespans and accelerating aging phenotypes, suggesting the importance of the MDM2-p53 praxis to the aging process [5].

However, p53's link to organismal aging may not be easily explainable just by the MDM2-p53 axis. MDM2 has only minor regulatory effects on the levels of p53 in *Heterocephalus glaber (*the naked mole rat). And, interestingly, *H. glaber* lives an average of 30 years compared to an average of 2-4 years for most rodents. This is thought to be due in part to a hyperstable p53–the source of this stability remains largely unknown [6,7]. In another case, the African elephant–*Loxodonta africana*–despite being predisposed to cancer due to prolonged UV-radiation and large body mass lives comparably long lives and displays a significantly lower frequency of cancer when compared to humans. The unique presence of 20 copies of p53 in their genome is thought to be responsible for this [8].

The relationship between p53 and organismal longevity is thus multifaceted: changes in DNA binding, changes in N-terminal, and increases in the number of isoforms are established structural and molecular features that increase lifespan. However, whether or not these structural properties and mechanistic differences are observed across a wider range of organisms–insights that could have implications for the development of

therapeutics for accelerated age-related phenotypes–is not clear. Considering the gaps in mapping out the mechanistic and structural relevance of p53 to cellular senescence and a multitude of changes in p53 that appear to correlate with longevity, investigating this relationship warrants a study of p53 orthologs in a broader evolutionary context. To address this, we develop a relative evolutionary scoring (RES) algorithm to comprehensively investigate the changes in p53 structure across organisms of various taxonomic orders and observed average lifespan to assess which residues and domains of aligned p53 sequences have evolutionary differences that could statistically explain differences in observed average lifespan.

Mapping out some mechanistic pathways of p53-induced cellular senescence across a broad sample of organisms could also be valuable to understanding the role of p53 in organismal aging. Several genes are implicated in the p53/p21 cellular senescence pathway, with some known to interact with p53, or p53 upstream regulator, following protein expression. Of interest to this study are the interactions between p53 and Smad2, Smad3, Rbl2, Npm1, MDM2, and Klf4; the interaction between MDM2 and Rpl11; and the interaction between Pras40 and Atk. These interactions either induce or inhibit cellular senescence: (a) p53 and Smad proteins: p53/Smads complex formation is required for the regulation of important tumor suppressive genes and/or cellular senescence regulatory genes. The tumor suppressor *GATA4*, which induces cellular senescence ectopically, loses this ability when Smad2 is knocked down while Smad3 complexes with p53 in its activation of the cellular senescence-inducing gene PAI-1 [9,10]. (b) p53 and Rbl2: Rbl2 is major pocket protein in the p53/p21 DNA-repair-induced cellular senescence pathway [11]. (c) p53 and Npm1: Npm1

regulates the stability and transcriptional activity of p53 via direct interaction. It inhibits p53-mediated senescence [12,13]. (d) p53 and MDM2: MDM2 ubiquitinates p53 for degradation, and thus inhibits cellular senescence abilities of the p53/p21 pathways [14]. (e) p53 and Klf4: Klf4 physically interacts with p53, causing activation of the p21 promoter [15]. (f) MDM2 and Rpl11: Rpl11 is a ribosomal protein that cooperatively binds MDM2, disrupting its ubiquitinase activity and stabilizing p53; induction of p53-dependent senescence is averted upon co-depletion of Rpl11 in HeLa cells [16,17]. (g) Pras40 and Atk: Dual phosphorylation by Atk and mTORC1 of Pras40 results in negative regulation of the Rpl11-MDM2 pathway, suppressing p53-mediated senescence [18].

We use the PEPPI protein-protein interaction prediction algorithm to assess the likelihood of interactions between these protein orthologs across organisms in the order Primates and Perciformes with varying average lifespans. Altogether, this study elucidates some structural and mechanistic diversity in p53-induced cellular senescence regulation across organisms and builds on evidence that this induction may be implicated in organismal aging.

Results

We developed a RES algorithm to score the evolutionary changes of single residues of p53 sequences. The algorithm uses a position weight matrix and global background frequencies of amino acids observed [19,20]. 15 sequences within the taxonomic orders Primates, Rodentia, Artiodactyl, Perciformes, Cetacean, and Carnivora were first aligned in the MEGA software package using the MUSCLE alignment algorithm and then scored using RES [21]. A seventh set of sequences was aligned and scored: the top three longest-lived organisms from each of the aforementioned orders. Following residue-wise scoring of each sequence in the alignments, we calculated an r^2 between the 15 (or 18 for the cross-order alignment) scores at each position and the observed lifespans of the 15 (or 18) organisms. We used this r^2 to predict whether a residue could be longevity-associated, termed RES-predicted longevity-associated residue (RPLAR). After the removal of any outlier(s), we used a cutoff r^2 of 0.3 to determine RPLARS. The RPLARs describe the residue of the unaligned ortholog of the longest-lived organism in each order. Specifications regarding the scoring algorithm and determination of this r^2 value can be found in the Material and Methods section.

In-order alignment revealed varying RPLARs across orders

We found no RPLAR in the artiodactyl alignment, with differences in RES where $r^2 >= 0.3$ explainable only by the presence of a single outlier, *Hippopotamus amphibius kiboko*, the longest-lived organism within the alignment. The Carnivora alignment contained four RPLARs: residues 66, 70, 135, and 326 (with respect to the *Ursus*

maritimus ortholog). The Cetacean alignment had two RPLARS, both in the

DNA-binding domain: residues 255 and 290 (with respect to the *Balaenoptera physalus*

ortholog). We found four RPLARs in the Perciformes alignment, occupying regions of

the N-terminal and DNA-binding domains: residues 30, 40, 136, and 278 (with respect

to the *Labrus bergylta* ortholog). The Primate alignment contained five RPLARS across

the N-terminal and downstream the DNA-binding domains: residues 10, 40, 51, 289,

and 296 (with respect to the *Homo sapiens* ortholog). Finally, four RPLARS were found

in the Rodentia alignment: residues 12, 59, 208, and 359 (with respect to the

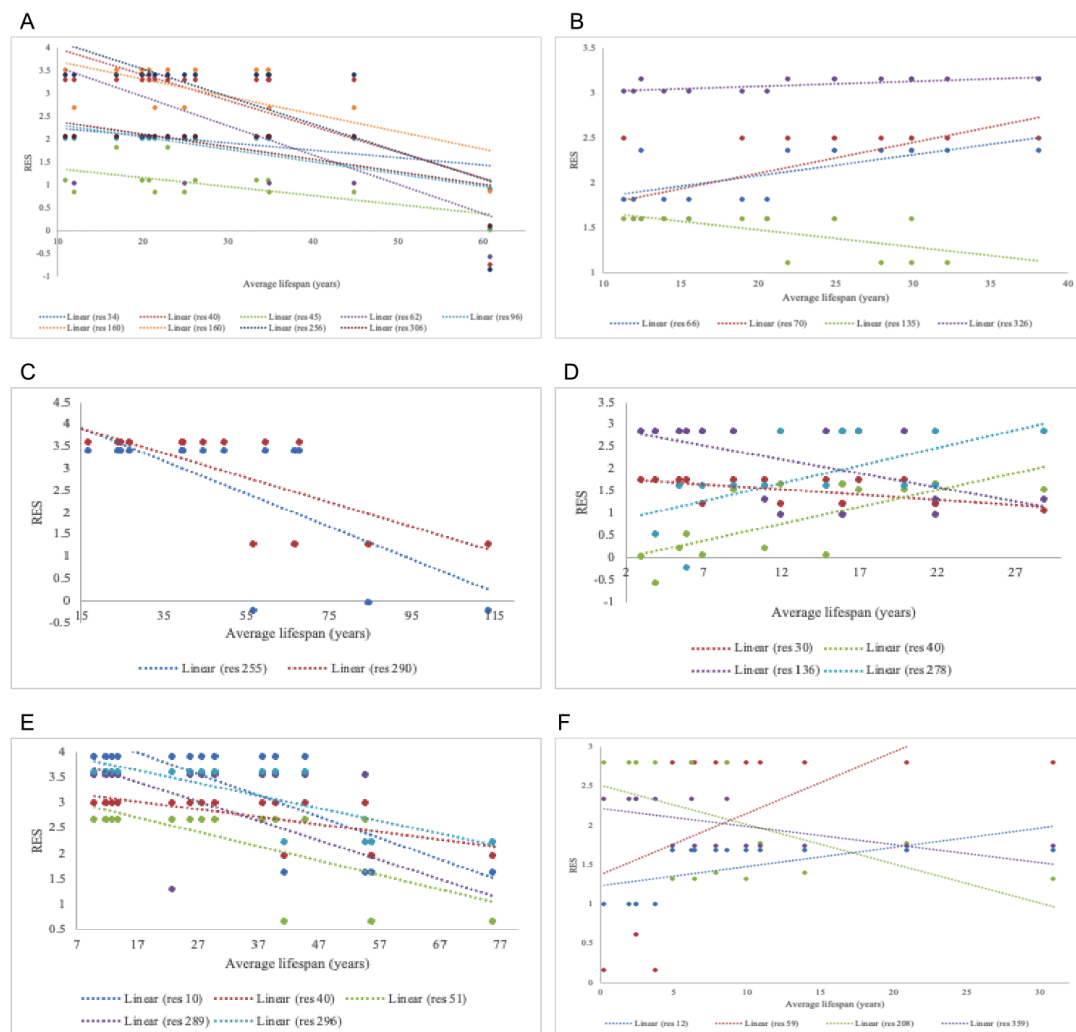*Heterocephalus glaber* ortholog). Fig 1 displays these findings.

Fig 1. Linear plot of in-order changes in RES of RPLARS and non-RPLARs. (A) The linear difference in Artiodactyl alignment is explainable only by an outlier, thus non-RPLARs. (B) RES changes in Carnivora RPLARS: residues 66 (r^2=0.50), 70, (r^2=0.43), 135 (r^2=0.37), and 326 (r^2=0.50). (C) RES changes in Cetaceans RPLARS: residues 255 (r^2=0.47), and 290 (r^2=0.53). (D) RES changes in Perciformes RPLARS: residues 30 (r^2=0.33), 40 ((r^2=0.53), 136 (r^2=0.32), and 278 (r^2=0.40). (E) RES changes in Primates RPLARS: residues 10 (r^2=0.59), 40 (r^2=0.43), 51 (r^2=0.43), 289 (r^2=0.31), and 296 (r^2=0.59). (F) RES changes in Rodentia RPLARS: residues 12 (r^2=0.36), 59 (r^2=0.32), 208 (r^2=0.33), and 359 (r^2=0.37).

Cross-order alignment predicted most RPLARS in N- and C-terminals

Next, we conducted an alignment and RES scoring to assess the relationship between sequence diversity and observed lifespan in a cross-order context. This alignment involved the p53 orthologs of the organism with the top three highest observed average lifespans. The alignment predicted 10 RPLARs, with most of them occurring in the N- and C-terminals: residues 39, 63, 66, 69, 71, 73, 122, 305, 325, and 350 (with respect to the *Balaenoptera physalus* alignment). The greatest difference is RES for most of these RPLARs is observed between the Cetacean and Rodentia orthologs, which have the greatest difference in average lifespan (~40 years) across the six orders. The RPLARs in this alignment also contained a greater number of amino acid substitutions that are of functionally different classes. Fig 2 depicts this.
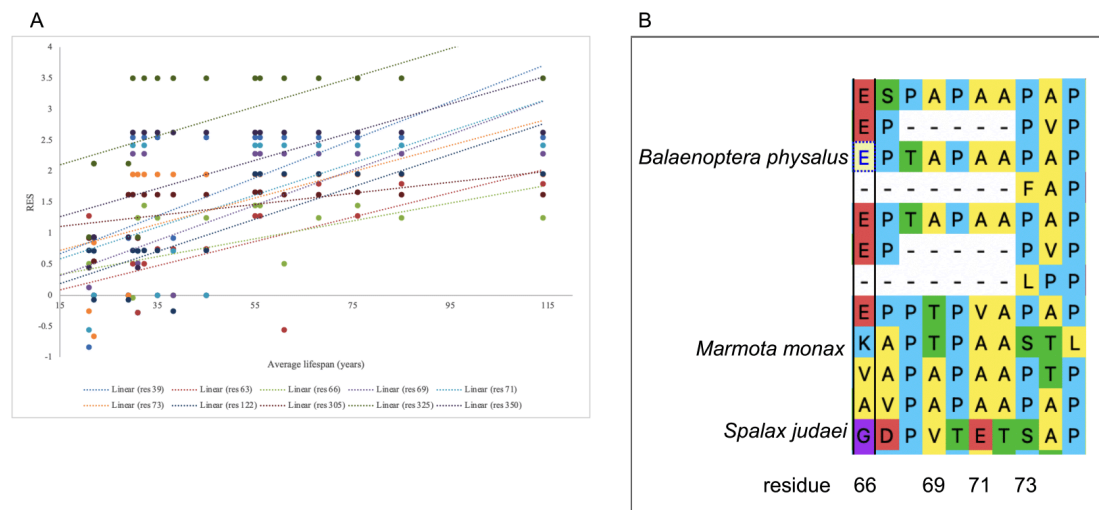
Fig 2. Cross-order linear plot of RPLARs and alignment. (A) RES changes in p53 orthologs of top three longest-lived organisms in each order: residue 39 (r^2=0.42), 63 (r^2=0.46), 66 (0.35), 69 (0.45), 71 (r^2=0.32), 73 (r^2=0.33), 122 (r^2=0.64), 305 (r^2=0.33), 325 (r^2=0.37), 350 (r^2=0.40). (B) Alignment of four of the ten RPLARS, showing amino acid changes between the longest-lived organism *Balaenoptera physalus* (a Cetacea) and two of the shortest-lived organisms *Marmota monax* and *Spalax judaei* (Rodents) in the alignment.

To ascertain the extent to which mutation at these identified residues (in both the in-order and cross-order alignment) affects the function of p53, we used the Sorting Intolerant from Tolerant (SIFT) algorithm. SIFT uses a sequence homology-based method to predict the likelihood of a residual substitution affecting a protein's functionality. A SIFT score of 1 suggests that a mutation is not predicted to affect functionality while a score less than 0.05 is predicted to be deleterious; a score between these ranges is predicted to be tolerated. We compared missense mutations of p53

sequences belonging to the longest and shortest-lived organisms. If the two sequences had the same residue at a particular point, the organism with the next shortest lifespan and a residual change was tested against the longest-lived organism. The average SIFT score of the RPLARs in each order is as follows: Primates had an average score of 0.816, Carnivora had an average score of 0.715, Rodentia had a score of 0.53, Artiodactyl had an average score of 0.888, Perciformes had an average score of 0.438, and Catacean had an average score of 0.325. The average SIFT score for RPLARs from the cross-order alignment was 0.519. None of the mutations had a deleterious effect on p53 function. See Fig 3 for details of individual RPLAR SIFT scoring.
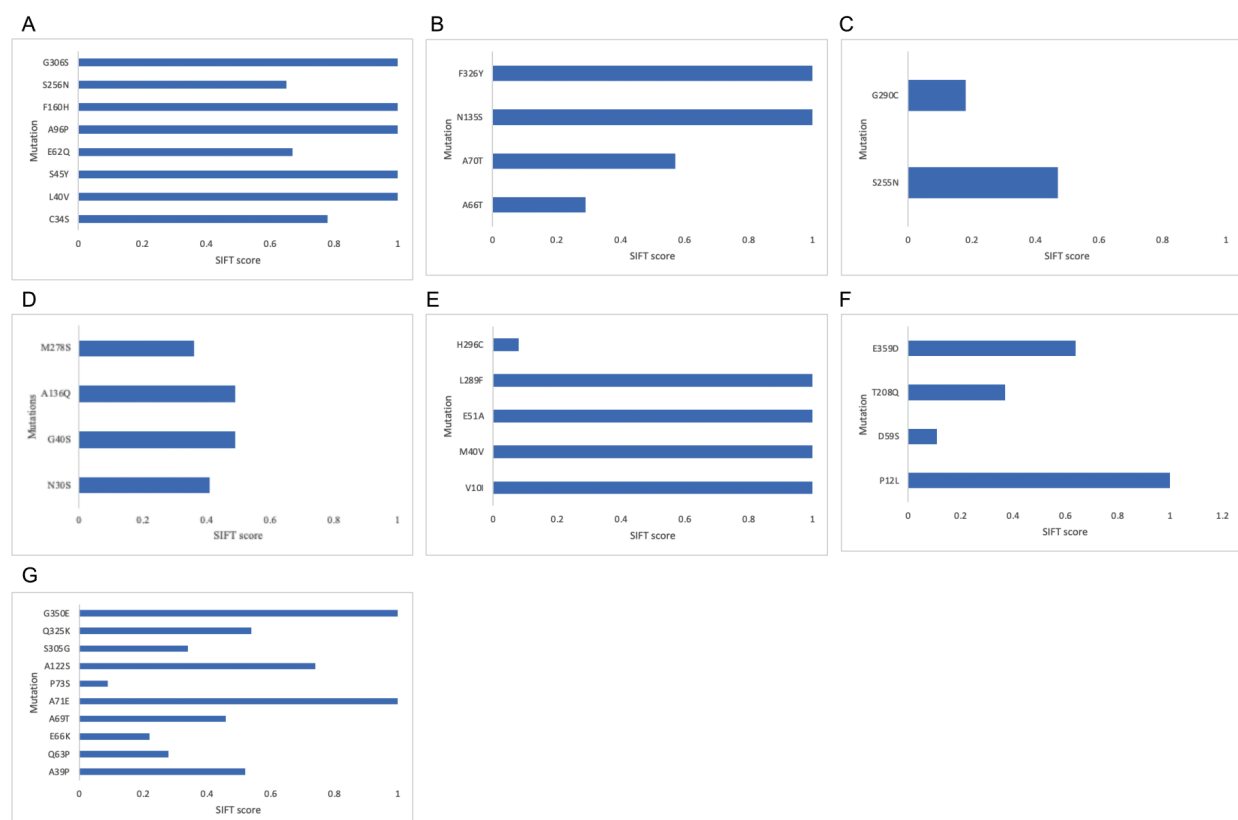

Fig 3. SIFT predictions of mutations at RPLARs and non-RPLARs. (A) SIFT scoring of the non-RPLARs in the Artiodactyl alignment: mutation S256N has the lowest score

of 0.65. (B) SIFT scoring of the RPLARs in the Carnivora alignment: mutation A66T had the lowest SIFT score of 0.29. (C) SIFT scoring of the RPLARs in the Cetaceans alignment: mutation G290C had the lowest SIFT score of 0.18. (D) SIFT scoring of the RPLARs in the Perciformes alignment: mutation M278S had the lowest SIFT scoring of 0.36. (E) SIFT scoring of the RPLARs in the Primates alignment: mutation H296C had the lowest SIFT score of 0.08. (F) SIFT scoring of the RPLARs in the Rondentia alignment: mutation D59S had the lowest SIFT score of 0.11. (G) SIFT scoring of the RPLARs in the cross-order alignment: mutation P73S had the lowest SIFT score of 0.09.

We then used the RES and SIFT algorithms and analyses to assess the effect of potential disruption of the MDM2-praxis on the lifespans of organisms whose orthologs were used in the cross-order alignment. Using the human p53 ortholog, we assessed the r^2 values, classification of amino acid change, and SIFT scoring of nine residues involved in the MDM2-p53 axis: residues S15, T18, S20, K370, K372, K373, K381, K382, and K386. Mutation at the tenth residue, P72, has been demonstrated to decrease lifespan in some human populations [22]. The average r^2 (modeling the relationship between RES and average lifespan) was 0.10, with residue 72 having the highest r^2 of 0.18. Four of the ten positions involved deletion (residues 370, 372, and 373) or no change in amino acid (residue 381), so six missense mutations were scored in SIFT. Most of the mutations proved to be deleterious, with an average SIFT score of 0.17. Mutation at residue 72 had the highest tolerance score of 0.57. In the N-terminal residues, the *Pan troglodytes* ortholog differed from that of the *Homo sapiens* while

orthologs from all aligned Perciformes (*Labrus berylta*, *Perca fluvialitis*, and *Epinephelus coioides*) differed from that of *Homo sapiens* in the C-terminal residues (see Fig 4).
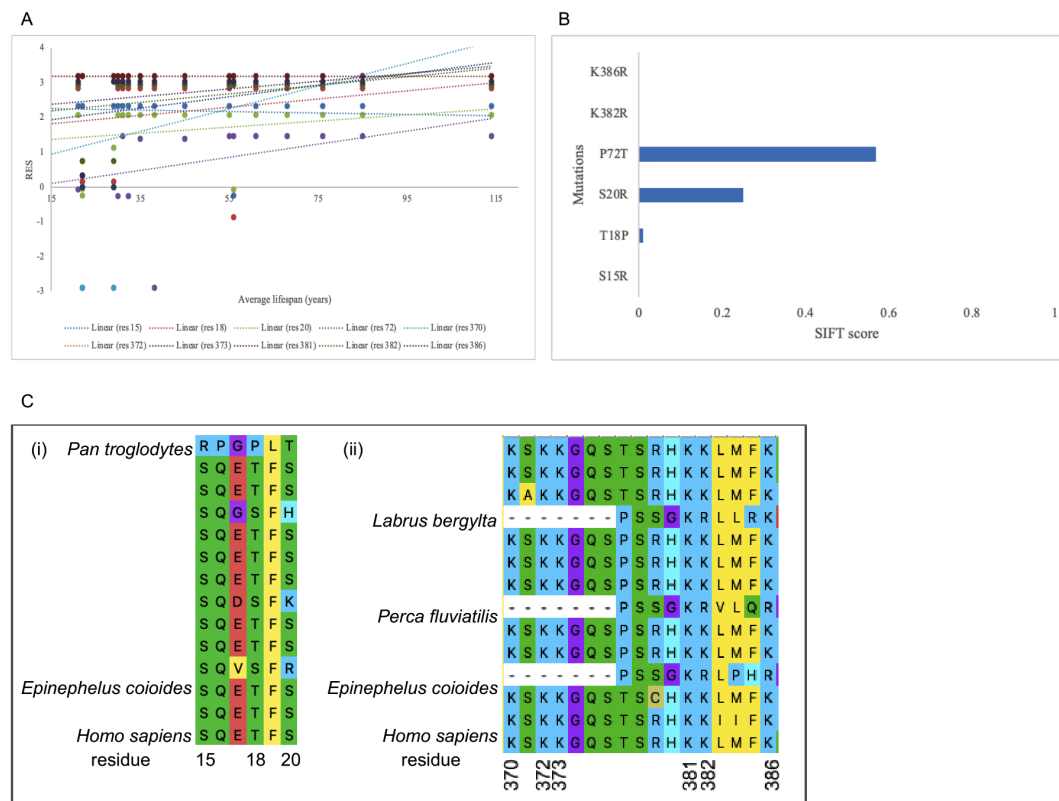

Fig 4. Cross-order linear plot, SIFT scoring, and alignment p53 residues involved in longevity or MDM2 regulation. (A) RES changes in p53 orthologs of top three longest-lived organisms in each order: residues 15, 18, 20, 381 (all with $r^2 < 0.1$), 372, 373, 382 (all with $r^2 = 0.15$), 72 ($r^2=0.18$), and 386 ($r^2=0.11$). (B) ASIFT scoring of the RES in the cross-order alignment: mutations S15R, K382R, and K386R all have the lowest SIFT score of 0.0. (C) Alignment of the MDM2-linked residues, showing amino acid changes at the (i) N-terminal residues primarily between the *Homo sapiens* and *Pan troglodytes* orthologs and (ii) C-terminal residues between the *Homo sapiens* and Perciformes orthologs.

Likelihood of p53-mediated senescence interactions varied within and across orders

Several protein-protein interactions are implicated in the induction and/or inhibition of p53-mediated cellular senescence. Studies show that disruption of the p53-MDM2 induces senescence and p53-null environments may rescue aging phenotypes [2]. Considering the established role of senescence in aging, we hypothesize that the likelihood of interaction between senescence-inducing protein-protein interactions should decrease with increasing lifespan; and that the likelihood of interaction between senescence-inhibiting protein-protein interactions should increase with increasing lifespan. We used PEPPI, which combines structural and sequence information, functional association data, and a naive Bayesian classifier model to predict the likelihood of interactions (log(LR)) between eight pairs of p53 orthologs in orders Primates and Perciformes: 4 cellular senescence-inducing and 4 senescence-inhibiting interactions [23].

Cellular senescence-inducing interactions

For Primates, the p53-Rbl2 and MDM2-Rpl11 interactions followed our hypothesis–average lifespan increased as log(LR) decreased, though r^2 values of 0.06 and 0.13 suggest that the relationship may not be significant. Results from all of the other senescence-inducing interactions modeled in PEPPI opposed the hypothesis and instead displayed an increase in lifespan as log(LR) increased, with the highest r^2 value being 0.40 for interaction between p53-Klf4 in primates. Fig 5 displays these results.

For both p53-Klf4 and MDM2-Rpl11 interactions, we displayed the predicted interacting residues in PyMOL and found residual differences that may contribute to the difference in log(LR) observed. In the p53-Rbl2 interaction, residue H115 of p53 interacts with residue R46 of Rbl2. Alignment of the p53 sequences reveals that the ortholog of one of the shortest shortest-lived Primates, *Theropithecus gelada*, uniquely has a lysine residue at aligned position 115. In the MDM2-Rpl11 interaction of the shortest-lived organism (and that with the highest log(LR)), Rpl11 is predicted to interact with MDM2 from several residues in its N-terminal. For the organisms with the lowest log(LR) and two of the highest average lifespans, *Pan troglodytes* and *Pan paniscus*, Rpl11 is predicted to interact with MDM2 via approximately 30 residues downstream its N-terminal domain (see Fig 6).
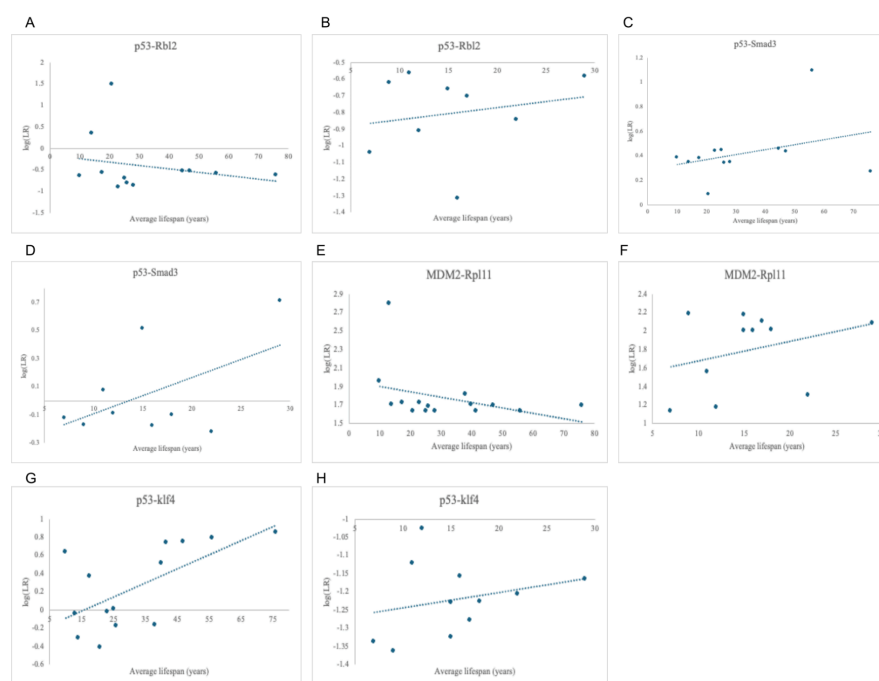

Fig 5. Relationship between log(LR) and average lifespan in senescence-inducing interactions. (A) Negative correlation of p53-Rbl2 in Primates (r^2 = 0.06). (B) Positive

correlation of p53-Rbl2 in Perciformes (r^2 = 0.04). (C) Positive correlation of p53-Smad3 in Primates (r^2 = 0.11). (D) Positive correlation of p53-Smad3 in Perciformes (r^2 = 0.28). (E) Negative correlation of MDM2-Rpl11 in Primates (r^2 = 0.13). (F) Positive correlation of MDM2-Rpl11 in Perciformes (r^2 = 0.09). (G) Positive correlation of p53-Klf4 in Primates (r^2 = 0.40). (H) Positive correlation of p53-Klf4 in Perciformes (r^2 = 0.07).
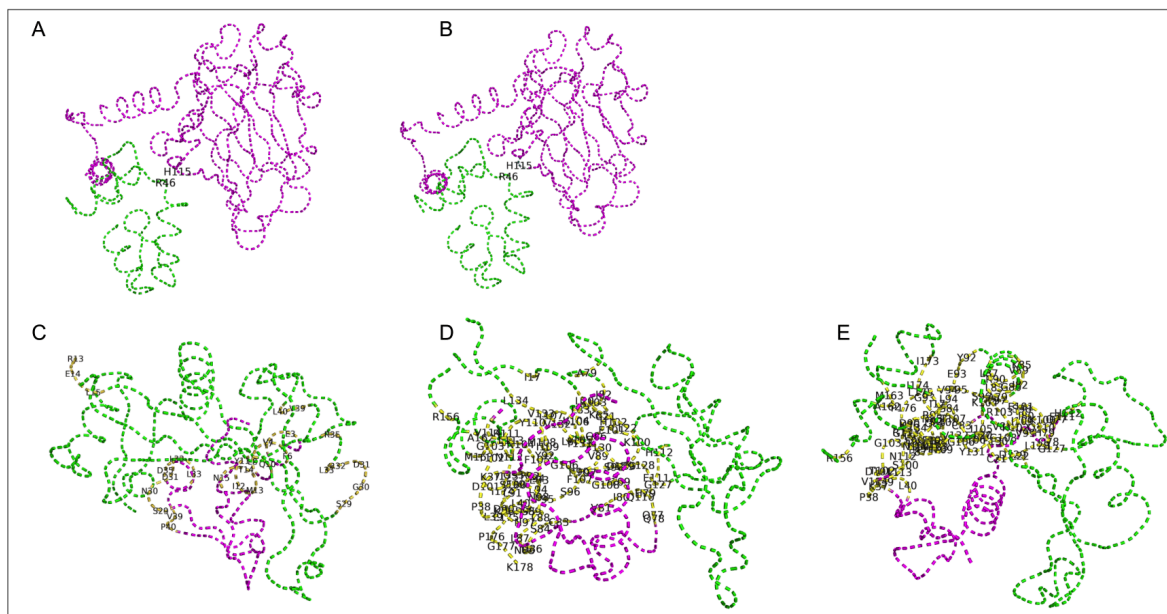
Fig 6. PyMOL-predicted interacting residues. (A) Model of human p53-Klf4 ortholog with interaction between p53 His115 and Klf4 Arg46. (B) Model of *Pan troglodytes* (Chimpanzee) p53-Klf4 ortholog with interaction between p53 His115 and Klf4 Arg46. (C) Model of *Carlito Syrichta* (Philippine tarsier) MDM2-Rpl11 ortholog with Rpl11 interacting from its N-terminal residues. (D) Model of *Pan troglodytes* MDM2-Rpl11 ortholog with Rpl11 interacting from downstream its N-terminal residues. (D) Model of *Pan paniscus* (Bonobo) MDM2-Rpl11 ortholog with Rpl11 interacting from downstream its N-terminal residues.

Cellular senescence-inhibiting interactions

For both Primate and Perciformes, the p53-Smad2 and p53-MDM2 interactions conformed to our hypothesis with the greatest strengths: average lifespans increase with increasing log(LR) with r^2 values of 0.13 and 0.12 for the p53-Smad2 interactions and r^2 values of 0.21 and 0.13 for the p53-MDM2 interactions, respectively. The likelihood of Pras40-Akt and p53-Npm1 interactions in both the Primates and Perciformes are virtually constant or have low r^2 values (< 0.03) across average lifespans (Fig 7). PyMOL found no detected interacting residues in any of the P

Fig 7. Relationship between log(LR) and average lifespan in senescence-inhibiting interactions. (A) Positive correlation of p53-Smad2 in Primates (r^2 = 0.13).(B) Positive correlation of p53-Smad2 in Perciformes (r^2 = 0.12). (C) Positive correlation of Pras40-Akt in Primates (r^2 = 0.007). (D) Negative correlation of P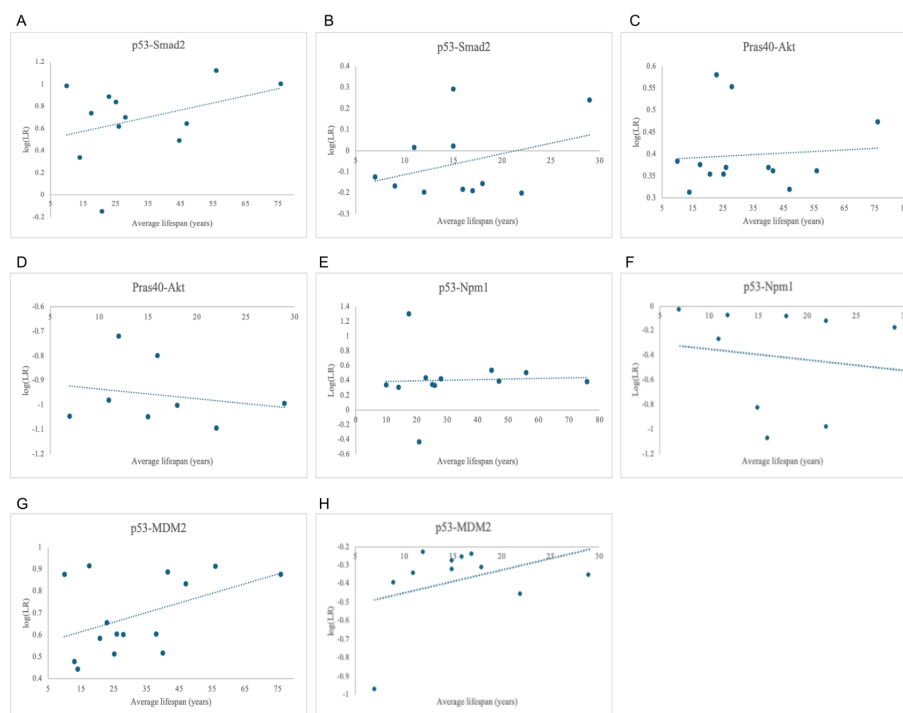ras40-Akt in Perciformes (r^2 = 0.044). (E) Positive correlation of p53-Npm1 in Primates (r^2 = 0.001). (F) Negative correlation of p53-Npm1 in Perciformes (r^2 = 0.02). (G) Positive correlation of p53-MDM2 in Primates (r^2 = 0.21). (H) Positive correlation of p53-MDM2 in Perciformes (r^2 = 0.13).

For all the senescence-inhibiting interactions, the average log(LR) for Primates WAS greater than that for Perciformes–with all of the Primate interactions predicted as interacting while those in Perciformes were predicted as non-interacting. The difference in the senescence-inducing interactions between the Primates versus Perciformes differed from this observation. On average, the p53-Rbl2 interaction for the Primates orthologs was predicted as non-interacting, similar to the Perciformes ortholog with a higher non-interacting likelihood. Overall, the differences in the likelihood of senescence-inducing interactions between Primates and Perciformes are significantly less than those of senescence-inhibiting interactions (Fig 8).
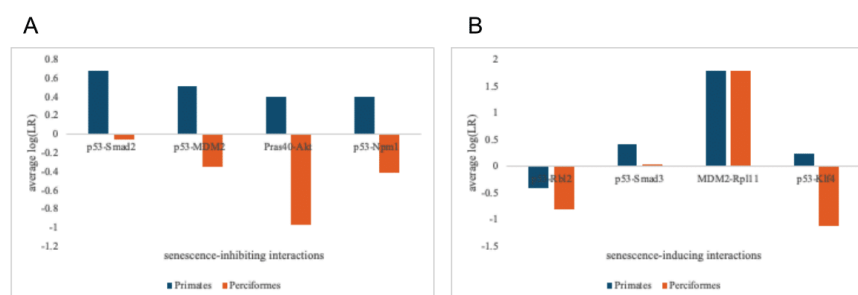
Fig 8. Average log(LR) for the 8 interactions. (A) Average log(LR) for senescence-inhibiting interactions in Primates (n=12-15) and Perciformes (n=8-11). (B) Average log(LR) for senescence-inducing interactions in Primates (n=12-15) and Perciformes (n=9-11).

Discussion

Senescence regulatory activities by the p53 tumor suppressor protein have been linked to aging on the molecular level, and a few studies have implicated this link to organismal aging–mainly in mouse models. In this study, we created a relative evolutionary scoring (RES) approach that scored aligned p53 sequences in search of residues that display a relatively strong statistical relationship ($r^2 >= 0.3$) to differences in observed lifespans across organisms in six taxonomical orders. In addition, we examined eight protein-protein interactions (of Primates and Perciformes orthologs) that are implicated in the p53/p21 cellular senescence pathway. We used the PEPPI protein-protein predictor to assess the likelihood of interaction of four senescence-inducing and four senescence-inhibiting interactions.

p53 structural diversity linked to varying lifespans

Our RES findings suggest that the p53 tumor suppressor residues that influence the difference in observed lifespan vary across the six taxonomical orders. The Artiodactyla alignment contained no RPLAR; the Carnivora and Rodentia alignments both contained two RPLARs in their N-terminal, one in their DNA-binding domains, and another in their C-terminal; the Perciformes alignment contained two RPLARs in both their N-terminal and DNA-binding domain while the Primates alignment contains three RPLARs in the N-terminal and two in its DNA-binding domains. The Cetacean alignment uniquely contains two in its DNA-binding domain.

This difference in the domains in which RPLARs are found suggests that cellular senescence may be variably regulated across orders. In mouse models, the N-terminal

contains the binding site for the most well-documented inhibitor of p53–the mouse double minute two (MDM2) protein. Disruption of the MDM2-p53 axis in some mice induces premature senescence and thus accelerated aging [24]. We hypothesize that p53 orthologs in Carnivora, Perciformes, Primates, and Rodentia may depend on similar inhibitory mechanisms at their N-terminal residues in regulating cellular senescence. Differences in the p53 DNA-binding domain of Cetaceans have been linked to longevity [4]. Our results support this finding and suggest that DNA binding may also be an important regulator of longevity in all five orders with RPLARS in the DNA-binding domain. It is well known that p53 binds and upregulates several senescence-associated genes, hence, it is feasible why the DNA-binding domain may be structurally important in the regulation of longevity. Also, the N-terminal of p53 interacts with the DNA-binding domain to regulate the protein's stability [25]. This may explain the presence of RPLARS in the N-terminal of p53 orthologs in Carnivora, Perciformes, Primates, and Rodents. We propose that the p53 ortholog in organisms in these orders may depend on interactions between their DNA-binding and N-terminal residues in their regulation of cellular senescence. SIFT scoring qualifies missense mutations of all RPLARS as tolerated, but an average scoring of 0.56 (on a scale of 0-1.0, where 1.0 predicts a change with the greatest tolerance) suggests that some mutations are causing some functional change. Whether or not these changes are affecting the regulation of longevity needs to be further explored.

Unlike the in-order alignments, from which most RPLARs are predicted to be in the DNA-binding domain, the cross-order alignment predicts most RPLARS to be in the N-

and C-terminals. In a cross-order context, changes in the N-terminal may be linked to p53's downstream regulation by factors such as post-transcriptional modifications or inhibitory oncoproteins such as MDM2. Changes in the C-terminal may also be crucial to p53's regulation of longevity. Mouse p53 binds DNA and regulates genes as a tetramer [26]. The C-terminal is crucial for the tetramerization and stabilization of p53-DNA complexes, thus it is feasible that amino acid substitutions that significantly alter the chemical environment of C-terminal residues may affect p53's ability to tetramerize and stably bind DNA [27].

The effects of the disruption of the MDM2-p53 axis on organismal longevity remain unclear, though some of our results point to its involvement. p53 residues S15, T18, and S20 serve as sites of phosphorylation by either ATM or Chk2. Phosphorylation of these residues causes MDM2 dissociation from p53, which enhances p53 transcriptional activities [28]. These residues are virtually constant in the cross-order alignment, with the only amino acid change observed in the *Pan troglodytes* (Chimpanzee) ortholog. While the S15R and T18P mutations (the human ortholog has S15, T18, and the chimpanzee ortholog has R15, P18) are predicted to be deleterious, the chimpanzee remains one of the longest-lived Primates. Our RES algorithm does not classify these sites as RPLARs as they both have $r^2 < 0.1$. We propose two hypotheses for this observation: (1) these MDM2-linked residues in the N-terminal may have no or negligible effect on organismal aging and other sites within the N-terminal may be involved in MDM2-p53 association or/and (2) these MDM2-linked residues in the N-terminal have an effect on organismal aging and whether accelerated aging

phenotypes is observed (as a result of disruption to the MDM2-p53 axis) depends on downstream mechanisms such as the genomes' ability to clear senescent microenvironments. Residue 72 follows, partly, the first hypothesis: its RES most strongly explains the difference in average lifespans, and the P72 SNP increases the lifespan of individuals by 6% over a 12-year period compared to R72 [22]. Interestingly, the R72 SNP influences increased phosphorylation of p53 S15 and transactivation of p21 compared to P72 [29]. Thus, the P72 SNP could help maintain the MDM2-p53 axis and inhibit the p53/p21 cellular senescence pathway, and thus reduce accelerated aging. Still, MDM2 regulation of p53-mediated cellular senescence appears to conflictingly depend on S15 phosphorylation. Our N-terminal RPLARS may play a similar role in this regulation.

The RES changes in the C-terminal residues have higher r^2 values ($r^2 > 0.1$) across the aligned orthologs than those in the N-terminal, though they are not RPLARs. Residues K370, K372, K373, K381, K382, and K386 are sites for acetylation by CBP/p300 and ubiquitination by MDM2 [30]. Acetylation of these residues is thought to prevent ubiquitination by MDM2, thus enhancing p53 stability [31]. As MDM2 ubiquitination at these residues triggers p53 degradation, there is a constant play between MDM2 and CBP/p300 to degrade or stabilize p53. The Perciformes in the alignment uniquely contain either a deletion or arginine substitution at these residues, and all missense mutations are predicted to be deleterious by SIFT. Out of the six orders, and besides Rodentia, Perciformes have the lowest average lifespan. The changes in their sequence at these acetylation and ubiquitination residues appear to have a substantial effect on the MDM2-p53 axis and potentially their longevity. With potential disruption to

acetylation, p53 orthologs of Perciformes may not be appropriately stabilized when needed, and could potentially expose their genome to excessive damage, predisposing them to shorter lifespans [32]. And, with potential disruption to ubiquitination, p53 levels may remain largely unregulated, triggering uncontrolled activities such as the p53/p21 pathway which could enhance the accumulation of senescent cells, and thus accelerate aging.

Mechanistic diversity in induction and inhibition of p53-mediated cellular senescence

From the PEPPI predictions, the observed likelihood of senescence-inducing and senescence-inhibiting protein-protein interactions across primates and Perciformes reifies the diversity in p53 regulation of senescence that our RES study suggests. The established role of cellular senescence in driving aging at the molecular level and findings that mouse models with unregulated p53 display accelerated aging phenotypes, led us to the hypothesis that, on an organismal level, the relative likelihood of p53-senescence-regulating protein-protein interactions may be implicated in aging. Our results of 8 such interactions complicate this. For the interactions that are found to induce p53-mediated cellular senescence, only the p53-Rbl2 and MDM2-Rpl11 interactions conformed, with low r^2 values of 0.06 and 0.13 respectively, to our hypothesis that average lifespan would increase if the likelihood of interaction decreases. Similarly, for the interactions that are found to inhibit p53-mediated cellular senescence, the p53-MDM2 and p53-Smad2 interactions conformed with the hypothesis that an increase in log(LR) would be observed as average lifespans

increase. While the study predicts the p53-MDM2 interaction to be the strongest inhibitor p53, the consistently low r^2 (<0.5) between log(LR) and average lifespan suggests that the mere likelihood of induction or inhibition of a single pair of protein-protein interactions may not fully or accurately explain observed differences in average lifespans within a taxonomic order. Considering the established complexity of p53 interactions in a multitude of physiological and metabolic pathways, its role in senescence within an order may be more integrative and compounded. Additionally, results from the Primates and Perciformes p53-Smad3, p53-Klf4, and Perciformes MDM2-Rpl11 interactions (which all deviate from our initial hypothesis) suggest that cellular senescence, through these senescence-inducing these pathways, could be enhancing longevity. Cellular senescence is a requisite for a plethora of physiological processes such as wound healing and embryonic development, and hence why its induction may be necessary [33].

While the intra-order relationship between the likelihood of interaction and the average lifespan is quite subtle, this relationship when viewed from a cross-order context appears much clearer. For the senescence-inhibiting interactions, the Primate orthologs have significantly higher likelihoods of interaction than the Perciforme orthologs. We speculate that a feature of Primates that evolved longer lifespans (compared to Perciformes) is the ability to inhibit p53-mediated cellular senescence. Perciformes compete better in senescence-inducing interactions, though Primates still average better likelihoods of interactions. This, coupled with the established "good" and "bad" roles of cellular senescence suggests that organisms may need to create an

appropriate balance between induction and inhibition of senescence to maintain healthy aging.

Conclusions & Future Directions

We found variations in the p53 tumor suppressor residues in Primates, Rodentia, Artiodactyl, Carnivora, Cetaceans, and Perciformes that could be linked to organismal aging. Our RES algorithm prioritizes p53's direct binding capabilities, but studies have demonstrated that regulation of and by p53 could be mediated allosterically [34]. The results from our PEPPI study give us new insight to begin mapping out a p53-mediated cellular senescence proteomic landscape. Several computational and experimental approaches could be employed to assess the effect(s) of this diversity in both the structure and mechanisms of p53 across organisms. Site-directed mutagenesis of p53 orthologs from organisms in each order, followed by an affinity binding assay could be conducted. If mutations are determined to cause significant functional change, then model organisms could be created with specific strains of p53, and their lifespans compared to those with the wild type. As Cetaceans and Rodents have the greatest difference in RES in the cross-order alignment, *in vitro* binding assays could be carried out to quantify binding between known N-terminal interacting proteins such as MDM2 and the p53 orthologs of rodents and cetaceans. To compare the degree of tetramerization of p53 in organisms of these orders, vapor diffusion could be employed to crystallize orthologs from these organisms. Molecular dynamics could also be used to assess potential allosteric pathways that our RPLARs may be implicated in as well as to

gain insight into the thermodynamic and mechanistic changes that occur as a result of RPLAR mutations.

Tumor suppressor p53-mediated cellular senescence is variably mediated across orders. Longevity may be linked to these variations via p53's tight balancing of induction and inhibition of cellular senescence. Further investigation of p53's role in this balancing play is required. Altogether, our study reifies the established complexity of p53's regulating of longevity and provides crucial molecular information that, through experimental verification, could enable the development of various models of p53 regulation of aging, ultimately making way for therapeutic targets to treat various accelerated aging-related diseases.

Materials and Methods

Observed Average Lifespan Data and Protein sequences

The observed average lifespan for each organism was obtained from the Animal Diversity Web (https://animaldiversity.org/; accessed on 13 January 2024), the AnimalLifeExpectancy (AnAge, UMICH, Max Planck, PanTHERIA, Arkive, UKC, AKC) databases as well as from Smithsonian National Zoo Database. Organism in each order was selected such that the order had a wide range of observed average lifespans. Protein sequences in RES, SIFT, and PEPPI studies for all organisms were obtained from the UniProt database (https://www.uniprot.org/; accessed on 15 October 2023) or the NIH's GenBank database (https://www.ncbi.nlm.nih.gov/genbank/; accessed 12 October 2023). See Tables 1-6 in the Supporting Information section for a list of the organisms, their observed average lifespans, and UniProt or GenBank accession numbers for protein sequences used throughout the study.

RES algorithm

Using the MUSCLE algorithm, p53 sequences were aligned by taxonomical order, and then the position weight matrix and background frequency values were calculated from each alignment. The position weight matrix is calculated by first counting the frequency of each amino acid (or gap) at every position in the alignment, then normalizing the count to the probability that a particular amino acid will be found at a particular position in the alignment. Included in this count of frequency is a pseudo-count to avoid a count

of zero–an occurrence unlikely in naturally occurring protein sequences. We then calculated a corresponding dictionary of the overall (background) frequency of each amino acid (or gap) in the alignment. Including background frequency information in multiple sequence scoring algorithms improves scoring and identification of functional sites. Following this, we used our position weight matrix and background frequencies to score each position of individual aligned sequences by taking the log odds ratio of observed frequency to background frequency. Log-odds scoring has been used in most pair-wise scoring, as it formalizes differentiating between more functional and less functional positions [35]. We used the MUSCLE default gap opening and extension penalties of -2.90 and 0, respectively in our scoring. Link to RES github repository can be found in the Supporting Information section.

Assessing the functional significance of RES scoring

With respect to the observed average lifespan, a coefficient of determination (r^2) was calculated using Excel's CORREL and POWER functions for each residual position. This r^2 is used to determine the fraction of the observed lifespan that is explainable by the difference in RES scoring at that position. An $r^2 > 0.3$ was hypothesized to predict a residue as longevity-associated. We used a combination of the relative r^2 values across all residues and the frequency of amino acid changes observed at each position in estimating this r^2 cutoff. The average r^2 of each position across all six in-order alignments was found to be 0.03, with most positions having conserved residues across the aligned orthologs. We observed that positions with r^2 of about 0.2 had amino acid

substitutions, though the substitution was often limited to a single outlier. We therefore selected for an r^2 of or greater than 0.3 and then checked the RES at those positions for outliers. If no outlier was found, we determined that that position (relative to longest-lived ortholog) was an RPLAR and reported that r^2. If an outlier was found, we removed the outlier from that position's sample and recalculated the r^2, again using a cutoff of 0.3 to determine if a residue was an RPLAR.

To assess the functional correctness of this hypothesis, we employed SIFT [36]. We compared missense mutations of p53 sequences belonging to the longest and shortest-lived organisms. If the two sequences had the same residue at a particular point, the organism with the next shortest lifespan and a residual change was used in the prediction. Accession numbers of the p53 ortholog of the longest-lived organism in each order can be found in S1-S6 Tables in the Supporting Information section. Missense mutations in the ortholog of (one of the) shortest-lived organisms in each order is determined from MEGA alignment.

PEPPI: predicting the likelihood of p53-induced cellular senescence protein-protein interactions

PEPPI, developed by the Zhang Lab at the University of Michigan Medical School, effectively uses structural and sequence similarity, functional association data, and the Naive Bayesian classifier model to predict the likelihood of interactions between proteins [13]. This study scored protein-protein interactions using its web server [23]. PEPPI runs were conducted on the interactions between p53 and Smad2, Smad3, Rbl2,

Npm1, MDM2, and Klf4; the interaction between MDM2 and Rpl11; and the interaction between Pras40 and Atk of the Prtimates and Perciformes orthologs. Accession numbers of the sequences used can be found in S1 and S2 Tables of the Supporting Information section.

PyMOL: visualizing protein-protein interaction predictions

PEPPI outputs a PDB model of predicted protein-protein interaction (or non-interaction). We used the InterfaceResidues program in PyMOL with default settings and arguments to display the predicted interacting residues of the model [37].

Acknowledgments

Supporting Information

Organism			Protein sequence accession numbers									
Scientific name	Common name	Average lifespan (years)	p53	Smad2	Smad3	Rbl2	Npm1	Rpl11	MDM2	Pras40	Akt	Klf4
Callithrix jacchus	Common marmoset	10	A0A2R8MYD9	A0A2R8M5L4	F7DCC1	U3DXJ5	F7FL37	U3EPN5	F6UPT1	F6RUS2	U3C443	F7IJX6
Carlito syrichta	Philippine tarsier	13	A0A1U7U5H4	/	/	/	/	A0A1U7TUA5	A0A3Q0DPE7	/	/	A0A1U7TCZ4
Microcebus murinus	Gray mouse lemur	14	A0A8B7H7E6	A0A8B7F143	A0A8C5YBL9	A0A8B7GYT6	A0A8C5YAS8	A0A8C5XZX6	A0A8C5V8R7	A0A8C6EKZ4	A0A8C5VV71	A0A8B7EFL3
Mandrillus leucophaeus	Drill	28	A0A2K6AAH4	A0A2K5ZHC1	A0A2K5YMS3	A0A2K5ZL30	A0A2K5YDB8	A0A2K5YMD0	A0A2K6A872	A0A2K6A7P6	A0A2K5ZJA3	/
Macaca fuscata fuscata	Japanese macaque	30	P61260	/	/	/	/	/	/	/	/	/
Sapajus apella	Tufted capuchin	40	A0A6J3I233	A0A6J3GBM2	A0A6J3F4R4	A0A6J3G130	A0A6J3GDU9	A0A6J3JQA4	A0A6J3IMI1	A0A6J3GQB8	A0A6J3GYY1	A0A6J3EU19
Gorilla gorilla gorilla	Gorilla	47	G3R2U9	G3QPV6	A0A2I2ZDG8	G3RZ75	A0A2I2YQY6	G3RWD2	A0A2I2ZWM5	G3S586	G3RB32	G3SJ37
Pan troglodytes	Chimpanzee	56	A0A2I3S1V8	H2QEH9	A0A2I3TN10	K7C590	A0A2J8LXX4	A0A2I3TKT2	H2R792	K7AMC0	K7AGW5	H2QXN2
Homo sapiens	Human	76	P04637	Q15796	P84022	Q08999	P06748	P62913	Q00987	Q96B36	P31749	O43474
Macaca mulatta	Indochinese rhesus macaque	26	P56424	F7CP27	A0A1D5Q1C9	A0A1D5QDE7	F7AWJ2	F6PJ30	G7N7L5	A0A5F8AIB7	G7MWI7	A0A5F8AGZ8
Macaca fascicularis	Crab-eating macaque	38	P56423	/	/	/	/	A0A2K5UHI1	A0A2K5W2P1	/	/	A0A2K5VB57
Pan paniscus	Bonobo	41.5	A0A2R9A5P4	/	/	/	/	A0A2R9AUR7	A0A2R9AQ86	A0A2R9CMW9	A0A2R9BZ66	A0A2R8ZF10
Saimiri boliviensis boliviensis	Black-capped squirrel monkey	17.5	A0A2K6SLC5	A0A2K6V827	A0A2K6SKP9	A0A2K6V4D2	A0A2K6UT13	A0A2K6V210	A0A2K6S797	A0A2K6UND0	A0A2K6SGS8	A0A2K6SJ96

Theropithecus gelada	Gelada	20.8	A0A8D2F964	A0A8D2GAI2	A0A8D2G920	A0A8D2FRL2	A0A8D2K0P5	A0A8D2EEE2	A0A8D2K6W8	A0A8D2E2Q4	A0A8D2F2J1	A0A8D2E5U5
Rhinopithecus bieti *	Black-and-white snub-nosed monkey	23	A0A2K6LYM5	A0A2K6KLL7	A0A2K6K5G6	A0A2K6JU68	A0A2K6MQI9	A0A2K6K899	A0A2K6KDN6	A0A2K6KJD1	A0A2K6KHG5	A0A2K6JXF0
Papio anubis	Olive baboon	25.2	A0A096P2R8	A0A096NP77	A0A096NMF6	A0A096NIB6	A0A2I3MVB3	UPI000440407B	A0A2I3NF10	A0A0A0MU05	A0A2I3N0A6	A0A8I5R2U0
Cebus imitator *	Panamanian white-faced capuchin	45	A0A2K5RMZ8	/	/	/	/	/	/	/	/	/
Pongo abelii *	Sumatran orangutan	55	A0A2J8RWD8	/	/	/	/	/	/	/	/	/
Chlorocebus sabaeus *	Green monkey	12	A0A0D9RG12	/	/	/	/	/	/	/	/	/

S1 Table. Primates included in the study.

Organisms in order Primates included in the RES, SIFT, and/or PEPPI studies, their average lifespans, and UniPro or NCBI GenBank's protein accession numbers. * indicates those organisms whose p53 sequences are used in alignment for RES study.

Organism			Sequence accession numbers									
Scientific name	Common name	Average lifespan (years)	p53	Smad2	Smad3	Rbl2	Npm1	Rpl11	MDM2	Pras40	Akt	Klf4
Thunnus albacares *	Yellowfin tuna	9	XP_044196743.1	UPI001C4B2943	UPI00054C1478	UPI001CF64C10	/	UPI001C4D5AE3	UPI001CF6DDC0	/	/	UPI001CF6E266
Perca flavescens *	Yellow perch	12	A0A484CCM0	UPI00106EAF7A	A0A484DP09	A0A484D3R4	A0A484CM55	A0A484CRN0	A0A484BZ23	A0A6A5ENB6	A0A484C4T4	A0A484CJE2

Dicentrarchus labrax	European seabass	15	A0A8C4EKX1	A0A8C4E8G4	A0A8C4F4T0	A0A8P4KC99	A0A8C4I739	UPI0021F50FAC	A0A8C4DZ38	A0A8C4DEU5	A0A8C4DG29	A0A8C4HU78
Platichthys flesus*	European flounder	15	O12946	UPI002DB75018	/	/	/	UPI0011C10C13	UPI002DB897B8	/	/	UPI002DBCCB49
Sander lucioperca*	Zander	16	A0A8C9ZEJ7	A0A8D0D734	A0A8C9ZTJ9	A0A8D0CS09	A0A8C9XKY4	A0A8D0AAC8	A0A8C9XZT3	A0A8C9YHW4	A0A8C9XJN6	A0A8C9XNT1
Scomber scombrus*	Atlantic mackere	17	UPI002DD90AFB	UPI002DD915F3	/	UPI002DD91C6B	/	UPI00016333A1	UPI002FEBFDE1	/		UPI002DD90CB4
Perca fluviatilis*	European perch	22	A0A6A5F0Y3	A0A6A5EE76	A0A6A5FEG0	A0A6A5FA52	A0A6A5ESY6	A0A6A5ELS6	A0A6A5DZX5	/	A0A6A5DQU5	A0A6A5EH34
Epinephelus coioides*	Orange-spotted groupe	22	F8RKR1	/	/	/	A0A1D8V787	/	/	/	/	/
Labrus bergylta*	Ballan wrasse	29	A0A3Q3GRI3	UPI000F31D7C5	A0A3Q3MUV6	A0A3Q3LLZ5	A0A3Q3LSC0	UPI000F30F9F7	A0A3Q3FQT2	A0A3Q3E1S6	A0A3Q3GN09	A0A3Q3G1D1
Anabas testudineus*	Climbing perch	7	A0A3Q1JCZ8	A0A7N6BK16	A0A3Q1J1S9	A0A3Q1IKN7	A0A7N6AAM7	A0A3Q1IK23	A0A3Q1JLB4	A0A3Q1JP30	UPI00194B08E9	A0A3Q1J2Y9
Amphiprion percula	Orange clownfish	18	A0A3P8T0X9	A0A3P8RXC7	UPI000F387D83	/	A0A3P8SIS1	A0A3P8TH83	A0A3P8TU83	A0A3P8TXZ2	A0A3P8RL25	A0A3P8TF24

Scientific name	Common name	lifespan	p53 accessions									
Sparus aurata*	Gilt-head bream	11	A0A671VUB9	A0A671XQA2	A0A671TKP9	A0A671TJ72	A0A671TUQ4	A0A671YTZ8	A0A671Y7M9	A0A671XJ86	A0A671XJ74	A0A671VEU0
Acanthochromis polyacanthus*	Spiny chromis	6	A0A3Q1HGV2	/	/	/	/	/	/	/	/	/
Parambassis ranga*	Indian Glass Fish	5.5	A0A6P7K8V8	/	/	/	/	/	/	/	/	/
Sphaeramia orbicularis*	Orbiculate cardinalfish	4	A0A673CZK1	/	/	/	/	/	/	/	/	/
Salarias fasciatus*	Lawnmower blenny	3	A0A672G194	/	/	/	/	/	/	/	/	/
Thunnus maccoyii*	Southern bluefin tuna	20	UniRef100_UPI001C4B3AFC	/	/	/	/	/	/	/	/	/

S2 Table. Perciformes included in the study.
Organisms in order Perciformes included in the RES, SIFT, and/or PEPPI studies, their

average lifespans, and UniPro or NCBI GenBank's protein accession numbers. *

indicates those organisms whose p53 sequences are used in alignment for RES study.

Organism			Sequence accession numbers
Scientific name	Common name	Average lifespan (years)	p53
Mus musculus	House mouse	2	P02340

Cricetulus griseus	Chinese hamster	2.5	O09185
Mesocricetus auratus	Golden hamster	2.5	Q00366
Cavia porcellus	Guinea pig	5	Q9WUR6
Octodon degus	Common degu	6.5	A0A6P3F490
Chinchilla lanigera	Long-tailed chinchilla	10	A0A8C2YMX2
Castor canadensis	American beaver	11	A0A250YHC8
Spalax judaei	Middle East blind mole-rat	21	Q68VB0
Heterocephalus glaber	Naked mole-rat	31	G5B5D6
Mastomys natalensis	Natal multimammate mouse	0.25	P89002
Rattus norvegicus	Brown rat	3.8	P10361
Peromyscus maniculatus	Deer Mouse	8.7	A0A8C8TJT9
Meriones unguiculatus	Mongolian gerbil	6.3	Q920Y0
Ictidomys tridecemlineatus	Thirteen-lined ground squirrel	7.9	I3N5N2
Marmota monax	Groundhog	14	O36006

S3 Table. Rodents included in the study.

Organisms in order Rodentia included in the RES and SIFT studies, their average

lifespans, and UniPro or NCBI GenBank's protein accession numbers.

Organism			Sequence accession numbers
Scientific name	Common name	Average lifespan (years)	p53

Neovison vison	American mink	11.4	A0A8C7A9R2
Vulpes vulpes	Red fox	12	A0A3Q7TIN0
Canis lupus dingo	Dingo	14	A0A8C0K1L6
Nyctereutes procyonoides	Common raccoon dog	15.6	A0A811ZM26
Canis lupus familiaris	Dog	20.6	Q29537
Neomonachus schauinslandi	Hawaiian monk seal	25	A0A2Y9HEV7
Callorhinus ursinus	Northern fur seal	25	A0A3Q7NG00
Panthera leo	Lion	28	A0A8C8Y413
Felis catus	Cat	30	P41685
Ursus maritimus	Polar bear	38.2	A0A384BVC2
Zalophus californianus	California sea lion	30	A0A6J2FNY3
Lynx rufus	Bobcat	32.3	UPI001F1287F1
Enhydra lutris	Sea otter	19	A0A2Y9L4Q2
Panthera pardus	Leopard	22	A0A9V1DWE6
Suricata suricatta	Meerkat	12.5	A0A673UVH2

S4 Table. Carnivores included in the study.
Organisms in order Carnivora included in the RES and SIFT studies, their average

lifespans, and UniPro or NCBI GenBank's protein accession numbers.

Organism			Sequence accession number
Scientific name	Common name	Average lifespan (years)	p53
Lipotes vexillifer	Baiji	24	A0A340X8E6
Delphinapterus leucas	Beluga whale	40	Q8SPZ3
Tursiops truncatus	Common bottlenose dolphin	45	A0A2U4C2U9
Monodon monoceros	Narwhal	50	A0A4V5P9N3

Globicephala melas	Long-finned pilot whale	60	UPI00293D9E1D
Eubalaena glacialis	North Atlantic right whale	67	UPI002A5A2F50
Physeter macrocephalus	Sperm whale	68	A0A455C1G1
Balaenoptera musculus	Blue whale	85	A0A8C0DFA9
Balaenoptera physalus	Fin whale	114	A0A6A1Q3Q7
Balaenoptera acutorostrata	Common minke whale	57	A0A383YUA7
Lagenorhynchus albirostris	White-beaked dolphin	40	XP_059988824.1
Mesoplodon densirostris	Blainville's beaked whale	27	XP_059937197.1
Delphinus delphis	Short-beaked common dolphin	25	XP_059854544.1
Kogia breviceps	Pygmy sperm whale	17	XP_058904949.1
Phocoena phocoena	Harbour porpoise	13	XP_065753055.1

S5 Table. Cetaceans included in the study.

Organisms in order Catacean included in the RES and SIFT studies, their average

lifespans, and UniPro or NCBI GenBank's protein accession numbers.

Organism			Sequence accession number
Scientific name	Common name	Average lifespan (years)	p53
Ovis aries	Sheep	11	P51664
Sus scrofa	Wild boar	12	Q9TUB2
Muntiacus muntjak	Southern red muntjac	17	A0A5N3WLG9

Bos taurus	Cattle	20	P67939
Capra hircus	Goat	20.8	A0A452G0A3
Odocoileus virginianus texanus	Texas white-tailed deer	23	A0A6J0VGP1
Vicugna pacos	Alpaca	25	A0A6I9IU1
Bison bison bison	Plains bison	33.5	A0A6P3HQA5
Camelus bactrianus	Bactrian camel	35	A0A9W3H045
Hippopotamus amphibius kiboko	Hippopotamus	61	XP_057572051.1
Camelus dromedarius	Dromedary	45	A0A5N4D2L6
Bubalus bubalis	Domestic water buffalo	34.9	F6MDM8
Bos mutus grunniens	Wild yak	26.3	A0A0N7FDT7
Neophocaena asiaeorientalis asiaeorientalis	Yangtze finless porpoise	21.5	A0A341BQX3
Bos indicus	Zebu	20	P67938

S6 Table. Artiodactyles included in the study.
Organisms in order Artiodactyl included in the RES and SIFT studies, their average

lifespans, and UniPro or NCBI GenBank's protein accession numbers.

RES GitHub repository can be accessed at https://github.com/Romani20/RES. It

includes the RES program, installation instructions, and fasta files to score p53

sequences involved in study.

References

1. Qian Y, Chen X. Senescence Regulation by the p53 Protein Family. Methods Mol Biol Clifton NJ. 2013;965:37–61.

2. Wu D, Prives C. Relevance of the p53-MDM2 axis to aging. Cell Death Differ. 2018 Jan;25(1):169–79.

3. Chaib S, Tchkonia T, Kirkland JL. Cellular senescence and senolytics: the path to the clinic. Nat Med. 2022 Aug;28(8):1556–68.

4. Bartas M, Brázda V, Volná A, Červeň J, Pečinka P, Zawacka-Pankau JE. The Changes in the p53 Protein across the Animal Kingdom Point to Its Involvement in Longevity. Int J Mol Sci. 2021 Aug 7;22(16):8512.

5. Maier B, Gluba W, Bernier B, Turner T, Mohammad K, Guise T, et al. Modulation of mammalian life span by the short isoform of p53. Genes Dev. 2004 Feb 1;18(3):306–19.

6. Oka K, Yamakawa M, Kawamura Y, Kutsukake N, Miura K. The Naked Mole-Rat as a Model for Healthy Aging. Annu Rev Anim Biosci. 2023 Feb 15;11:207–26.

7. Deuker MM, Lewis KN, Ingaramo M, Kimmel J, Buffenstein R, Settleman J. Unprovoked Stabilization and Nuclear Accumulation of the Naked Mole-Rat p53 Protein. Sci Rep. 2020 Apr 24;10(1):6966.

8. Sulak M, Fong L, Mika K, Chigurupati S, Yon L, Mongan NP, et al. TP53 copy number expansion is associated with the evolution of increased body size and an enhanced DNA damage response in elephants. eLife. 5:e11994.

9. Gao L, Hu Y, Tian Y, Fan Z, Wang K, Li H, et al. Lung cancer deficient in the tumor suppressor GATA4 is sensitive to TGFBR1 inhibition. Nat Commun. 2019 Apr 10;10(1):1665.

10. Kawarada Y, Inoue Y, Kawasaki F, Fukuura K, Sato K, Tanaka T, et al. TGF-β induces p53/Smads complex formation in the PAI-1 promoter to activate transcription. Sci Rep. 2016 Oct 19;6(1):35483.

11. Helmbold H, Kömm N, Deppert W, Bohn W. Rb2/p130 is the dominating pocket protein in the p53–p21 DNA damage response pathway leading to senescence. Oncogene. 2009 Oct;28(39):3456–67.

12. Zarka J, Short NJ, Kanagal-Shamanna R, Issa GC. Nucleophosmin 1 Mutations in Acute Myeloid Leukemia. Genes. 2020 Jun 12;11(6):649.

13. Wong JCT, Hasan MR, Rahman M, Yu AC, Chan SK, Schaeffer DF, et al. Nucleophosmin 1, upregulated in adenomas and cancers of the colon, inhibits p53-mediated cellular senescence. Int J Cancer. 2013 Oct 1;133(7):1567–77.

14. Wu L, Maki C. MDM2: RING Finger Protein and Regulator of p53. In: Madame Curie Bioscience Database. Austin, TX: Landes Bioscience; 2000.

15. Yoon HS, Chen X, Yang VW. Krüppel-like Factor 4 Mediates p53-dependent G1/S Cell Cycle Arrest in Response to DNA Damage. J Biol Chem. 2003 Jan 24;278(4):2101–5.

16. Horn HF, Vousden KH. Cooperation between the ribosomal proteins L5 and L11 in the p53 pathway. Oncogene. 2008 Oct 2;27(44):5774–84.

17. Lindström MS, Nistér M. Silencing of Ribosomal Protein S9 Elicits a Multitude of Cellular Responses Inhibiting the Growth of Cancer Cells Subsequent to p53 Activation. PLOS ONE. 2010 Mar 8;5(3):e9578.

18. Havel JJ, Li Z, Cheng D, Peng J, Fu H. Nuclear PRAS40 couples the Akt/mTORC1 signaling axis to the RPL11-HDM2-p53 nucleolar stress response pathway. Oncogene. 2015 Mar;34(12):1487–98.

19. Xia X. Position Weight Matrix, Gibbs Sampler, and the Associated Significance Tests in Motif Characterization and Prediction. Scientifica. 2012;2012:917540.

20. Wang K, Samudrala R. Incorporating background frequency improves entropy-based

residue conservation measures. BMC Bioinformatics. 2006 Aug 17;7:385.

21.   Edgar RC. MUSCLE: a multiple sequence alignment method with reduced time and space complexity. BMC Bioinformatics. 2004 Aug 19;5:113.

22.   Ørsted DD, Bojesen SE, Tybjærg-Hansen A, Nordestgaard BG. Tumor suppressor p53 Arg72Pro polymorphism and longevity, cancer survival, and risk of cancer in the general population. J Exp Med. 2007 Jun 11;204(6):1295–301.

23.   Bell EW, Schwartz JH, Freddolino PL, Zhang Y. PEPPI: Whole-proteome Protein-protein Interaction Prediction through Structure and Sequence Similarity, Functional Association, and Machine Learning. J Mol Biol. 2022 Jun 15;434(11):167530.

24.   Gannon HS, Donehower LA, Lyle S, Jones SN. Mdm2-p53 signaling regulates epidermal stem cell senescence and premature aging phenotypes in mouse skin. Dev Biol. 2011 May 1;353(1):1–9.

25.   Natan E, Baloglu C, Pagel K, Freund SMV, Morgner N, Robinson CV, et al. Interaction of the p53 DNA-Binding Domain with Its N-Terminal Extension Modulates the Stability of the p53 Tetramer. J Mol Biol. 2011 Jun 10;409(3):358–68.

26.   Halazonetis TD, Kandil AN. Conformational shifts propagate from the oligomerization domain of p53 to its tetrameric DNA binding domain and restore DNA binding to select p53 mutants. EMBO J. 1993 Dec 15;12(13):5057–64.

27.   Laptenko O, Shiff I, Freed-Pastor W, Zupnik A, Mattia M, Freulich E, et al. The p53 C-Terminus Controls Site-Specific DNA Binding and Promotes Structural Changes within the Central DNA Binding Domain. Mol Cell. 2015 Mar 19;57(6):1034–46.

28.   Teufel DP, Bycroft M, Fersht AR. Regulation by phosphorylation of the relative affinities of the N-terminal transactivation domains of p53 for p300 domains and Mdm2. Oncogene. 2009 May 21;28(20):2112–8.

29.   Kung CP, Liu Q, Murphy ME. The codon 72 polymorphism of p53 influences cell fate following nutrient deprivation. Cancer Biol Ther. 2017 May 5;18(7):484–91.

30.   Dai C, Gu W. p53 post-translational modification: deregulated in tumorigenesis. Trends Mol Med. 2010 Nov;16(11):528–36.

31.   Tang Y, Zhao W, Chen Y, Zhao Y, Gu W. Acetylation Is Indispensable for p53 Activation. Cell. 2008 May 16;133(4):612–26.

32.   Barnes RP, Fouquerel E, Opresko PL. The impact of oxidative DNA damage and stress on telomere homeostasis. Mech Ageing Dev. 2019 Jan;177:37–45.

33.   Huang W, Hickson LJ, Eirin A, Kirkland JL, Lerman LO. Cellular senescence: the good, the bad and the unknown. Nat Rev Nephrol. 2022 Oct;18(10):611–27.

34.   Grinkevich VV, Vema A, Fawkner K, Issaeva N, Andreotti V, Dickinson ER, et al. Novel Allosteric Mechanism of Dual p53/MDM2 and p53/MDM4 Inhibition by a Small Molecule. Front Mol Biosci [Internet]. 2022 Jun 1 [cited 2024 Aug 2];9. Available from: https://www.frontiersin.org/journals/molecular-biosciences/articles/10.3389/fmolb.2022.823195/full

35.   Altschul SF, Wootton JC, Zaslavsky E, Yu YK. The Construction and Use of Log-Odds Substitution Scores for Multiple Sequence Alignment. PLOS Comput Biol. 2010 Jul 15;6(7):e1000852.

36.   Ng PC, Henikoff S. SIFT: predicting amino acid changes that affect protein function. Nucleic Acids Res. 2003 Jul 1;31(13):3812–4.

37.   Vertrees J. InterfaceResidues - PyMOLWiki [Internet]. 2009 [cited 2024 Jun 23]. Available from: https://pymolwiki.org/index.php/InterfaceResidues